Nmr Spectrum of *endo*-2-Dimethylphosphono-7-*anti*-1,4,5,6,7-pentachloro-5-bicyclo[2.2.1]heptene (8). The gross features of the spectrum have been described elsewhere.[4a] The ABM(XY) part of the spectrum was analyzed with the LAOCN3 program, giving the following results.

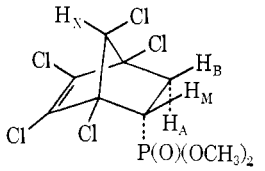

$J_{AB} = -12.3 \pm 0.03$ Hz	δ_A 231.4 ± 0.03 Hz
$J_{AM} = 5.0 \pm 0.03$ Hz	δ_B 269.4 ± 0.03 Hz
$^4J_{AX} = 1.4 \pm 0.04$ Hz	δ_M 312.4 ± 0.03 Hz
$J_{AY} = 17.1 \pm 0.05$ Hz	
$J_{BM} = 10.0 \pm 0.05$ Hz	
$J_{BY} = 8.6 \pm 0.05$ Hz	
$J_{MY} = -15.6 \pm 0.05$ Hz	

***syn*-7-Bromo-*endo*-2-dimethylphosphono-*exo*-2-hydroxybicyclo-[2.2.1]heptane (13).** A saturated solution of $NaOCH_3/CH_3OH$ (12 drops) was added to a mixture of *syn*-7-bromo-2-norbornanone[25] (1.404 g, 7.424 mmol) and dimethyl phosphonate (0.841 g, 76.4 mmol). After 48 hr at room temperature, the reaction mixture was chromatographed on a 50-g silica gel column. Successively eluted were (weight and eluent indicated) starting ketone (0.61 g, ether–methanol 9:1), and hydroxyphosphate **13** (1.05 g, 3.51 mmol, ether–methanol 8:2). Recrystallization from acetone afforded the analytical sample as white crystals: mp 132–133°; nmr ($CDCl_3$) 4.04 (d of m, 1 H, H_7, J_{PH} = 5.3), 3.87 and 3.83 (2d, 6 H, nonequiv CH_3OP, $^3J_{PH}$ = 10.4), 3.65 (s, 1 H, OH), 2.68 and 2.54 (broad s, 2 H, H_4 and H_1), 1.30–2.39 (complex m, 6 H). Irradiation of both H_1 and H_4 causes the collapse of the d of m, at 4.04 into a d.

Anal. Calcd for $C_9H_{16}BrO_4P$ (299.106): C, 36.14; H, 5.39; Br, 26.72. Found: C, 36.07; H, 5.38; Br, 26.84.

Compounds **3**, **5**, **9**,[4a] **14**, **15**,[4b,c] **16**, and **17**[4b] have been described elsewhere.

(25) L. H. Zalkow and A. C. Oehlschlager, *J. Org. Chem.*, **29**, 1625 (1964).

Electrostatic Force Treatment Based on Extended Hückel Molecular Orbitals. Structure and Reaction of Simple Hydrocarbons

Hiroshi Nakatsuji,* Takahira Kuwata, and Akihiro Yoshida

Contribution from the Department of Hydrocarbon Chemistry, Faculty of Engineering, Kyoto University, Kyoto, Japan. *Received February 21, 1973*

Abstract: Taking account of the intuitiveness and usefulness of the electrostatic force (ESF) theory proposed previously, we have exploited a "semiempirical" method for calculating electrostatic Hellmann–Feynman forces based on the extended Hückel MO's. Slater exponents in the calculation of force integrals were adjusted so that the resulting forces vanished in the equilibrium structure of ethane. First, bond lengths and force constants of various hydrocarbons were calculated. Although the results seem to be generally reasonable, there still remain some difficulties to be overcome for general utility. The mechanism of the internal rotation barrier of ethane was also examined. Second, the dimerization reaction of two methyl radicals was studied. Two reaction paths were examined. One is the approach of two planar methyl radicals and the other is the approach accompanying gradual change in HCH angles of each methyl radical. It is shown that the geometrical change of the reactants along the reaction path is essential for occurrence of the reaction. If two approaching methyl radicals are restricted to be planar, the dimerization reaction cannot proceed. From the analysis of force into atomic dipole (AD), exchange (EC), and extended gross charge (EGC) forces, an intuitive understanding of the nature of both molecular structure and chemical reaction becomes possible. Some important reorganizations of electron cloud (orbital following and preceding) in the course of nuclear displacement are pointed out for both problems. From these, the usefulness of the ESF concept is confirmed in the actual calculations.

In a previous series of articles,[1] one of us presented an electrostatic force (ESF) theory in which chemical phenomena are studied using force concepts (not energetics) on the basis of the electrostatic theorem of Hellmann and Feynman.[2]

$$\mathbf{F}_A = Z_A\left[\int \rho(\mathbf{r}_1)\mathbf{r}_{A1}/r_{A1}^3\, d\mathbf{r}_1 - \sum_{B(\neq A)} Z_B\mathbf{R}_{AB}/R_{AB}^3\right] \quad (1)$$

where $\mathbf{F}_A$ is the force acting on nucleus A of a system and the other notations are the same as those in paper I. The theorem permits a classical interpretation of the force acting on a nucleus A. Namely, the force is represented by the coulombic interaction of the positively charged nucleus A with the other positively charged nuclei B and with the negatively charged electron cloud $\rho(\mathbf{r}_1)$, which may be determined by some appropriate quantum-mechanical method.[3,4] Taking advantage of this physical simplicity and visuality, we derived three pictorial forces: the atomic dipole (AD), exchange (EC), and gross charge (GC) or extended gross charge (EGC) forces. This partitioning of force was shown to be very useful in studying molecular structure and chemical reaction.[1]

On the other hand, the calculations of electrostatic forces have been reported by several investigators.

(1) (a) H. Nakatsuji, *J. Amer. Chem. Soc.*, **95**, 345 (1973), which is called paper I; (b) *ibid.*, **95**, 354 (1973); paper II; (c) *ibid.*, **95**, 2084 (1973), paper III.

(2) H. Hellmann, "Einführung in die Quantenchemie," Deuticke, Vienna, 1937; R. P. Feynman, *Phys. Rev.*, **56**, 340 (1939).

(3) A. C. Hurley, "Molecular Orbitals in Chemistry, Physics and Biology," P.-O. Löwdin and B. Pullman, Ed., Academic Press, New York, N. Y., p 161; *Proc. Roy. Soc., Ser. A*, **226**, 170, 179 (1954).

(4) G. G. Hall, *Phil. Mag.*, **6**, 249 (1961).

Hurley compared the molecular orbital and valence bond wave functions from this standpoint.[3,5] Bader and Jones[6] developed and applied force concepts in order to obtain a better understanding of chemical binding. Bader and his coworkers[7] calculated density maps and forces acting on the nuclei of diatomic molecules from very accurate wave functions. Goodisman[8] and Sovers, *et al.*,[9] applied this concept to the barrier of internal rotation in ethane. Hirschfelder and Eliason[10] reported a very illuminating electrostatic picture for long-range interaction of two hydrogen atoms.

A defect of the electrostatic method is that the magnitude of the calculated forces is very sensitive to the accuracy of the approximate wave functions used.[7,8,11-13] Salem, Wilson, and Alexander[11] examined this problem and showed that the force is extremely sensitive to small density changes (*e.g.*, polarization) near atomic centers. If we use the "floating" atomic orbital (AO) basis proposed by Hurley,[3] the situation can be improved considerably, since the Hellmann–Feynman theorem is satisfied for this basis. The floating Gaussian orbitals extensively used by Frost[14] are very useful for this prupose.

In the present force calculations, semiempirical extended Hückel (EH) wave functions[15] are used. Such a wave function is very crude in light of the above discussion; the EH method neglects inner-shell electrons, the floating of AO basis, and the density polarization near the proton. It never satisfies Hellmann–Feynman theorem. A reason for using the EH MO's is in part that there are no sufficiently accurate wave functions for the present purposes. Since this situation is expected to continue for some time, it would seem worthwhile to develop a "semiempirical" method even for the "force" treatment. Inevitably, some parameters are introduced in this treatment in order to remedy *effectively* the defects of semiempirical MO's. Here, the exponents of Slater AO's are adjusted in the calculation of force integrals so that the structure of ethane is reproduced from this treatment.

We apply the above force treatment to calculation of molecular structure, vibrational force constants, and chemical reaction paths for some simple hydrocarbons. Another purpose of the study is to examine numerically the various results of the ESF theory hitherto presented.[1] We analyze the calculated forces into the AD, EC, and EGC forces and interpret the physical behavior of the system by means of these intuitive and pictorial forces.

Theoretical Background

Developing the density of electron cloud $\rho(\mathbf{r}_1)$ in eq 1 by means of the atomic orbital (AO) set $\{\chi_r\}$

$$\rho(\mathbf{r}_1) = \sum_{r,s} P_{rs}\chi_r(\mathbf{r}_1)\chi_s(\mathbf{r}_1) \tag{2}$$

we obtain

$$\mathbf{F}_A = Z_A\{\sum_{r,s} P_{rs}\langle\chi_r|\mathbf{r}_A/r_A^3|\chi_s\rangle - \sum_{B(\neq A)} Z_B\mathbf{R}_{AB}/R_{AB}^3\} \tag{3}$$

where P_{rs} is the density matrix element between AO's χ_r and χ_s. The first term represents the force due to the electrostatic interaction between nucleus A and the electron cloud of the system, which is called hereafter the electronic part. The second term is the internuclear repulsive force, which is called hereafter the nuclear part.

In paper I, eq 3 was rewritten with appropriate approximations as

$$\mathbf{F}_A = Z_A\{\sum_{r(\neq)s}^{A}\sum^{A} P_{rAsA}\langle\chi_{rA}|\mathbf{r}_A/r_A^3|\chi_{sA}\rangle + 2\sum_{B(\neq A)}\sum_{r}^{A}\sum_{s}^{B} P_{rAsB}\langle\chi_{rA}|(\mathbf{r}_A/r_A^3)_0|\chi_{sB}\rangle - \sum_{B(\neq A)}(Z_B - N_B)\mathbf{R}_{AB}/R_{AB}^3\} \tag{4}$$

where the net exchange force integral was defined by

$$\langle\chi_{rA}|(\mathbf{r}_A/r_A^3)_0|\chi_{sB}\rangle = \langle\chi_{rA}|\mathbf{r}_A/r_A^3|\chi_{sB}\rangle - \frac{1}{2}S_{rAsB}\langle s_B|\mathbf{r}_A/r_A^3|s_B\rangle \tag{5}$$

s_B is the s AO on atom B belonging to the same shell as χ_{sB}, N_B the gross atomic population,[16] and S_{rAsB} the overlap integral between χ_{rA} and χ_{sB}. The physical interpretation of eq 4 is simple.[1a] The first term, which is called the atomic dipole (AD) force, represents the attraction between nucleus A and the centroid of the polarized electron distribution belonging to the AO's of atom A. The second term is a sum of exchange (EC) forces, representing the attraction between nucleus A and the electron distribution piled up in the region between nuclei A and B. The third term, which is called the gross charge (GC) force, represents the electrostatic interaction between nucleus A and the gross charge on atom B, $Z_B - N_B$.[16]

Of these forces, only the GC force is approximate. However, as mentioned in paper I, the approximation can be eliminated by defining an extended gross charge (EGC) force as

$$\text{EGC force} = \mathbf{F}_A - (\text{AD force}) - (\text{EC forces}) \tag{6}$$

Then, all the AD, EC, and EGC forces are defined without integral approximations. The physical meaning of the EGC force is similar to that of the GC force except that the nuclear repulsive force is stressed more in the former than in the latter. In the present study, the partitioning of force into the AD, EC, and EGC forces is used. The sum of them (namely $\mathbf{F}_A$) is referred to as the total force.

(5) H. Shull and D. D. Ebbing, *J. Chem. Phys.*, 28, 866 (1958).
(6) (a) R. F. W. Bader and G. A. Jones, *Can. J. Chem.*, **39**, 1253 (1961); (b) *ibid.*, **41**, 586 (1963); (c) *J, Chem. Phys.*, **38**, 2791 (1963).
(7) (a) R. F. W. Bader and W. H. Henneker, *J. Amer. Chem. Soc.*, 88, 280 (1966); (b) R. F. W. Bader, W. H. Henneker, and P. E. Cade, *J. Chem. Phys.*, **46**, 3341 (1967); (c) R. F. W. Bader, I. Keaveny, and P. E. Cade, *ibid.*, **47**, 3381 (1967); (d) R. F. W. Bader and A. D. Bandrauk, *ibid.*, **49**, 1653, 1666 (1968); (e) P. E. Cade, R. F. W. Bader, W. H. Henneker, and I. Keaveny, *ibid.*, **50**, 5313 (1969); (f) P. E. Cade, R. F. W. Bader, and J. Pelletier, *ibid.*, **54**, 3517 (1971); (g) B. J. Ransil and J. J. Sinai, *ibid.*, **46**, 4050 (1967).
(8) J. Goodisman, *ibid.*, **45**, 4689 (1966); **47**, 334 (1967).
(9) O. J. Sovers, C. W. Kern, P. M. Pitzer, and M. Karplus, *ibid.*, **49**, 2592 (1968).
(10) J. O. Hirschfelder and M. A. Eliason, *ibid.*, **47**, 1164 (1967); see also, J. O. Hirschfelder and W. J. Meath, *Advan. Chem. Phys.*, **12**, 3 (1967).
(11) L. Salem and E. B. Wilson, Jr., *J. Chem. Phys.*, **36**, 3421 (1962); L. Salem and M. Alexander, *ibid.*, **39**, 2994 (1963).
(12) R. Yaris, *ibid.*, **39**, 863 (1963).
(13) For example, A. D. McLean and M. Yoshimine, *ibid.*, **47**, 3256 (1967); see also, W. H. Fink and L. C. Allen, *ibid.*, **46**, 3270 (1967).
(14) A. A. Frost, *J. Chem. Phys.*, **47**, 3707, 3714 (1967), and succeeding papers.
(15) R. Hoffmann, *J. Chem. Phys.*, **39**, 1397 (1963), and succeeding papers; see also, K. Fukui and H. Fujimoto, *Bull. Chem. Soc. Jap.*, **40**, 2787 (1967); G. Blyholder and C. A. Coulson, *Theor. Chim. Acta*, **10**, 316 (1968).
(16) R. S. Mulliken, *J. Chem. Phys.*, **23**, 1833 (1955).

Method of Calculation

The calculation of electrostatic force from eq 3 is divided into two steps. First is the calculation of density matrix P_{rs} and second is the calculation of force integrals, $\langle\chi_r|\mathbf{r}_A/r_A^3|\chi_s\rangle$. For the first step, the density matrix P_{rs} is calculated with the usual EH method. Taking account of its popularity, no modification is made for this method. For the second step, all the force integrals are calculated using Slater-type (ST) AO's for χ_r. A six-term Gaussian expansion method[17] is employed. The inner-shell electrons are treated as if they are absorbed into the nucleus. Thus, $Z_C = 4$ in the present calculation instead of 6.

A problem in the above treatment is that, if we calculate the forces acting on protons and carbons in ethane in its equilibrium geometry[18] with the use of usual orbital exponents ($\zeta_C = 1.625$, $\zeta_H = 1.0$) for ST-AO's,[19] large forces remain as shown in Table I.

Table I. Remaining Force in Equilibrium Structure of Ethane with Usual and Adjusted Orbital Exponent in the Force Integral Calculation (au)[a]

Force	Usual exponent $\zeta_C = 1.625$ $\zeta_H = 1.000$	Adjusted exponent $\zeta_C = 1.8629$ $\zeta_H = 1.0846$
F_C	0.1435	0.0000
F_H	0.0847	0.0006

[a] 1 au = 8.2377 mdyn.

Therefore, in calculating force integrals (not in the EH method), these orbital exponents were regarded as variable parameters[19] and adjusted so that the resulting forces in ethane vanished. Adjusted orbital exponents and the resultant forces are summarized in Table I. These adjusted orbital exponents are used for all the hydrocarbons studied in this paper.

The calculation of the AD and EC forces is based on the first and second terms of eq 4, and that of the EGC force is based on eq 6. The overlap integral appearing in the net exchange force integral (eq 5) is calculated using adjusted orbital exponents.

Bond Length and Force Constant

(i) General Results. An equilibrium structure calculated from the force method is, of course, the geometry for which the forces acting on all the nuclei vanish. However, in calculating the C–C and C–H lengths summarized in Table II, we varied only the carbon framework and the C–H distances, respectively, without destroying the symmetry of the molecule. Other parameters were held fixed at experimental values.[18] The third column gives the corresponding values obtained from the potential energy curves calculated simultaneously from the EH method. As seen from Table II, the results of the present calculation seem reasonable for linear hydrocarbons except for acetylene, for which the calculated force *vs.* C≡C distance curve was nonlinear. For cyclic hydrocarbons, the present results are always too large.

Table II. Equilibrium Bond Length of Hydrocarbons (Å)

Hydrocarbon	Bond	EH energy	Present	Expt[a]
Methyl radical	C—H	0.960	1.075	1.079
Methane	C—H	1.000	1.087	1.085
Ethane	C—C	1.964	(1.534)[b]	1.534
	C—H	1.043	(1.093)[b]	1.093
Ethylene	C=C	1.450	1.375	1.337
Butadiene[c]	C—C	1.790	1.550	1.483
	C=C	1.410	1.235	1.337
Acetylene	C≡C	0.844	1.560[d]	1.204
Cyclopropane	C—C	1.821	1.930	1.524
Cyclopentane	C—C	1.890	1.578	1.540
Benzene	C=C	1.501	1.732	1.397
	C—H	0.870	1.137	1.084

[a] Reference 18. [b] These values were referred to in adjusting the exponents of Slater AO's. [c] Mean value for cis and trans isomers. [d] The force *vs.* C≡C distance curve was nonlinear.

The force constants of the stretching vibrations are obtained from the slope of the force *vs.* coordinate curve at the point of vanishing force. They are summarized in Table III. The force *vs.* coordinate curves were approximately linear near the equilibrium points (small anharmonicity or small coupling between different inner coordinates), except for acetylene. Although for

Table III. Force Constant of Hydrocarbons (mdyn/Å)

Hydrocarbon	Vibration	EH energy	Present	Expt
Methyl radical	C—H Stretch	4.8	5.2	4.09[a]
Methane	C—H Stretch	8.7	4.4	5.39,[b] 4.76[c]
Ethane	C—C Stretch	5.7	4.7	4.57[b]
	C—H Stretch	6.5	4.2	5.35[b]
	∢HCH Bend	3.2	0.9	0.63[b]
Ethylene	C=C Stretch	6.7	2.1	7.40,[c] 11.72[d]
Butadiene[e]	C—C Stretch	3.7	5.5	
	C=C Stretch	6.2	6.2	
Acetylene	C≡C Stretch	12.6	*f*	15.59[a]
Cyclopropane	C—C Stretch	3.2	8.9	
Cyclopentane	C—C Stretch	10.4	3.8	
Benzene	C=C Stretch	12.8	6.4	5.46[c]
	C—H Stretch	6.2	4.9	4.56[c]

[a] G. Herzberg, "Molecular Spectra and Molecular Structure. II. Infrared and Raman Spectra of Polyatomic Molecules," Van Nostrand, Princeton, N. J., 1945. [b] G. E. Hansen and D. H. Denisson, *J. Chem. Phys.*, **20**, 313 (1952). [c] Y. Morino, Ed., "Kagaku Binran," Maruzen, Tokyo, 1966. [d] K. Machida, *J. Chem. Phys.*, **44**, 4186 (1966). [e] Mean value for cis and trans isomers. [f] The force *vs.* C≡C distance curve was nonlinear.

(17) K. O-ohata, H. Taketa, and S. Huzinaga, *J. Phys. Soc. Jap.*, 21, 2306, 2313 (1966); the expansion coefficient is used from the table given in R. F. Stewart, *J. Chem. Phys.*, **52**, 431 (1970).

(18) (a) L. E. Sutton, Ed., *Chem. Soc., Spec. Publ.*, **No. 11** (1958); **No. 18** (1965); (b) G. Herzberg, "Molecular Spectra and Molecular Structure, III. Electronic Structure of Polyatomic Molecules," Van Nostrand, Princeton, N. J., 1965.

(19) In the EH method, the usual Slater AO's (orbital exponents, $\zeta_C = 1.625$, $\zeta_H = 1.0$) are used for the calculation of overlap integrals which represent the bond-length dependence of the resonance integral in the manner (Wolfsberg–Helmholtz approximation).

$$H_{rs} = -(K/2)S_{rs}(Ip_r + Ip_s)$$

However, since the bond-length dependence of the resonance integral is not necessarily the same as that of the overlap integral, the AO basis of the EH method cannot always be identified with the usual Slater AO's. Linderberg has shown that the dependence of the resonance integral on internuclear separation may be expressed in some cases as

$$H_{rs} = \frac{h^2}{m}\frac{1}{R}\frac{dS}{dR}$$

where R is the internuclear separation: J. Linderberg, *Chem. Phys. Lett.*, **1**, 39 (1967); see also, C. C. J. Roothaan, *J. Chem. Phys.*, **19**, 1445 (1951).

the methyl radical, methane, and ethane the present values are satisfactory, those of ethylene and acetylene are disappointing. The reason seems to be due to the use of the same orbital exponents for both σ and π orbitals. For other molecules, the order of magnitude of the present values seems reasonable. Due to the lack of corresponding experimental values, fuller comparison with experiments is impossible.

As seen from the above results, the present method still has some defects to be overcome for general utility in bond length and force constant calculations. The present results obtained for the molecules which are considerably different from ethane (used as a standard molecule) are not improved in comparison with those obtained from the EH energy curves. Thus, we have limited the following discussion to ethane and related compounds.

(ii) **Analysis of Force.** Fuller understanding of the nature of chemical binding and on the origin of vibrational force constants is obtained from the analysis of force into the AD, EC, and EGC forces. Figure 1 shows two alternative analyses of the stretching force acting on carbon in ethane at various C–C distances, where the HCH angle of the methyl group was held fixed at the equilibrium value. A positive force acts to bind two methyl groups and a negative force is repulsive. The first analysis is based on the equation

$$\mathbf{F}_A = (\text{electronic part}) + (\text{nuclear part}) \quad (7)$$

As seen from Figure 1, the result of this analysis is trivial; the electronic part acts to bind two methyl groups, while the nuclear part is repulsive. The second analysis is based on the ESF theory and is expressed by

$$\mathbf{F}_C = [\text{AD force}] + [\text{EC(C–C, same } CH_3, \text{ different } CH_3) \text{ force}] + [\text{EGC force}] \quad (8)$$

where the EC(C–C) force is due to the electrons in the C–C bond region, the EC(same CH_3) force is due to the electrons in the C–H bond regions belonging to the same methyl group, and the EC(different CH_3) force is due to the interactions with other methyl hydrogens. For the origin of the C–C chemical binding, the EC(C–C) force is most important. Its dependence on the C–C distance is parallel with that of the electronic part. This is very natural from the meaning of the EC force.[1a] On the other hand, the EC(same CH_3) and EC(different CH_3) forces operate as repulsive forces. The former is due to the nearly tetrahedral configuration of each methyl group. The latter represents the nonbonded C–H interactions, which are similar to the repulsive interaction of two helium atoms. The contributions from the AD and EGC forces are very small. This may be reasonable from their physical meanings. Especially, the smallness of the EGC force means that the nuclear charge is nearly completely shielded by the gross electronic charge of the electron cloud around the nucleus. For the origin of the stretching force constant, the situation becomes a little more complicated. As seen from Figure 1, the sum of the positive slopes of the AD, EC(same CH_3, different CH_3), and EGC forces slightly offsets the negative slope of the EC(C–C) force. Such absence of dominant terms makes calculation of a stretching force constant rather difficult.

Figure 2 is the analyses of the bending forces acting on a carbon (Figure 2a) and a proton (Figure 2b) in

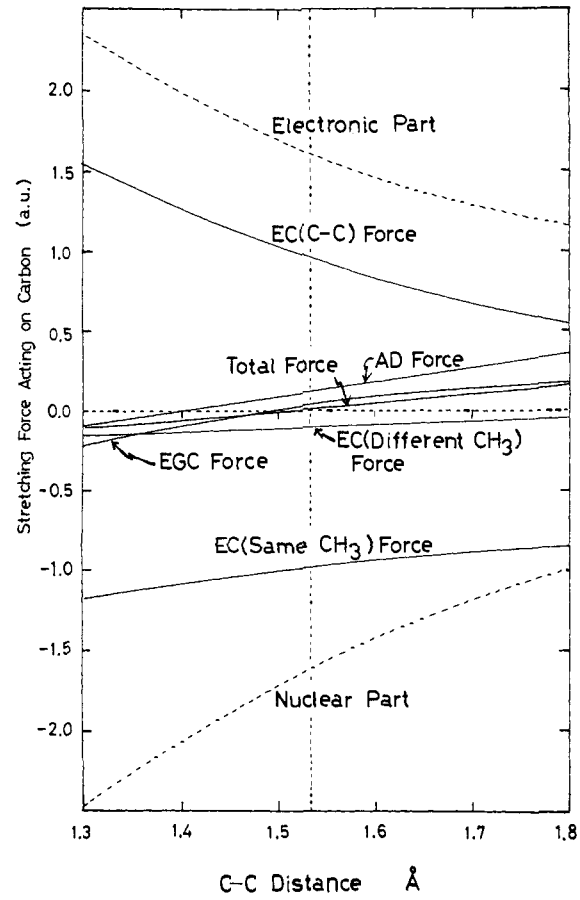

Figure 1. Analysis of the stretching force acting on the left-hand-side carbon in ethane in the direction of the C–C bond. The dotted curves show the analysis based on eq 7 and the real curves show the analysis based on eq 8. The vertical dotted line shows equilibrium C–C distance.

ethane. The directions of these forces are shown by arrows in the figures. For carbon, the analysis of force is based on eq 8, and for the proton, it is based on the following equation

$$\mathbf{F}_H = [\text{EC(H–C, other) force}] + [\text{EGC force}] \quad (9)$$

where the AD force is zero since polarization of the electron cloud near the proton is neglected in the EH method. The EC(H–C) force represents the EC force due to the H–C bond electrons. The EC(other) force is the sum of other (small) EC forces.

As seen from Figure 2a, the slope of the (total) force acting on the carbon is determined chiefly by that of the AD force. The sum of the slopes of the three EC forces (C–C, same CH_3, and different CH_3) almost vanishes. This is reasonable since the s–p hybridization at carbon (origin of the AD force) is very sensitive to the HCH angle. The EC(C–C) force is nearly independent of the HCH angle. On the other hand, for the force acting on the proton shown in Figure 2b, the slopes of the three component forces, EC(H–C, other) and EGC forces, are comparable. Among these, the EC(H–C) force arises from the incomplete following of the H–C bond orbital during the flapping displacement of protons from equilibrium positions.[1c,20] The EGC force arises mainly from interproton repulsions within the same methyl group.

(20) The generality of incomplete following and preceding of the local electron cloud in the course of nuclear displacement will be shown in the following paper: H. Nakatsuji, *J. Amer. Chem. Soc.*, in press.

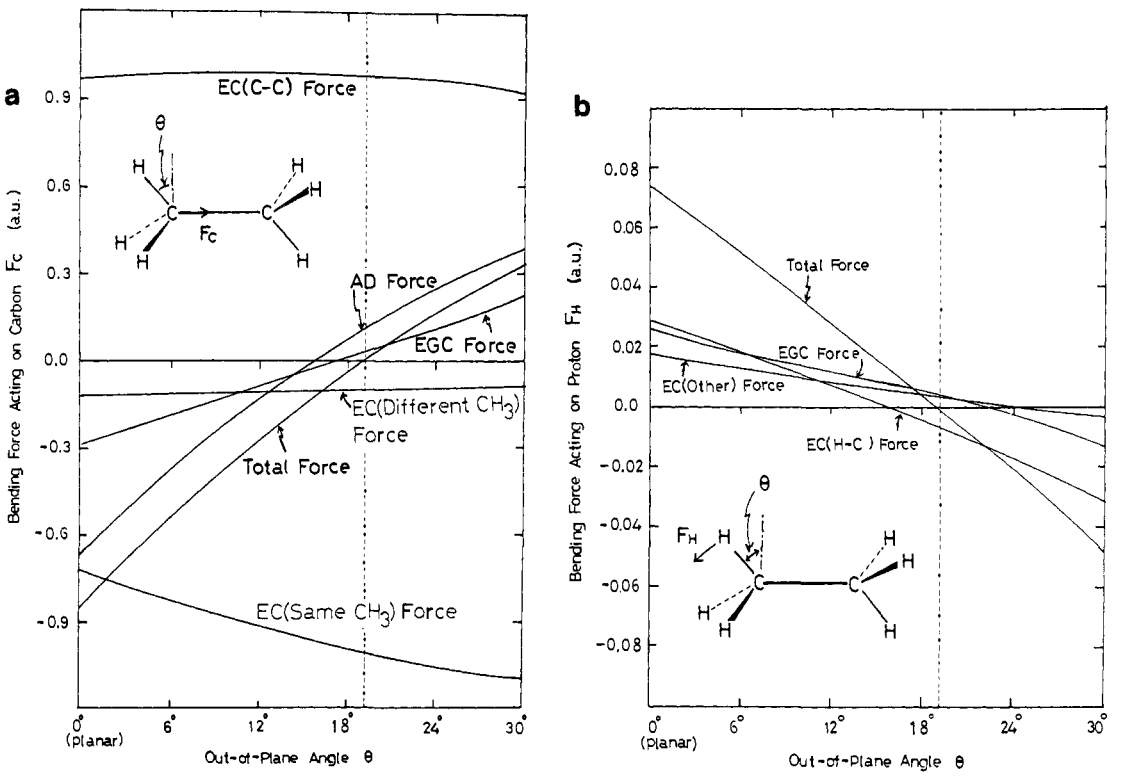

Figure 2. (a) Analysis of the bending force F_C acting on a carbon in ethane at various out-of-plane angles θ. The vertical dotted line shows the equilibrium angle. (b) Analysis of the bending force F_H acting on a proton in ethane at various out-of-plane angles θ. The vertical dotted line shows the equilibrium angle.

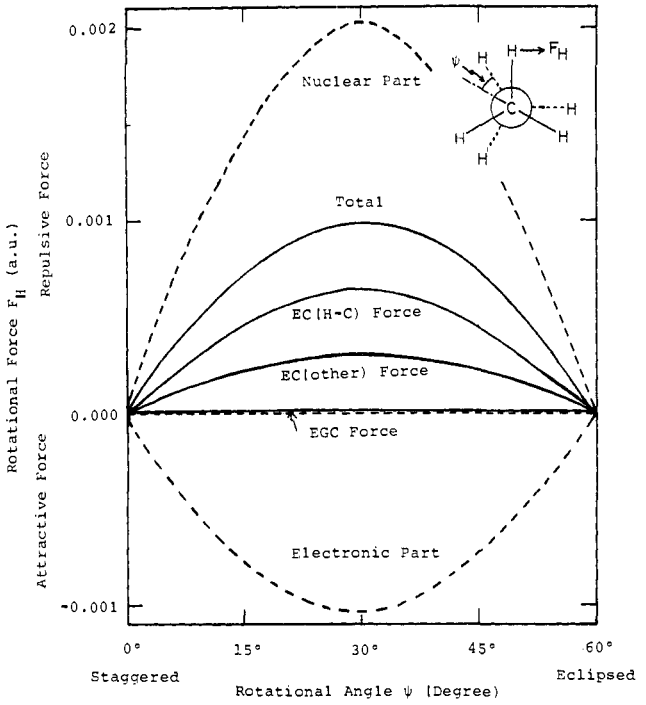

Figure 3. Analysis of the rotational force F_H acting on a proton in ethane at various rotational angles ψ. The dotted curves show the analysis based on eq 7 and the real curves show the analysis based on eq 9. A posive force corresponds to the restoring force to staggered form and its direction is shown by the arrow in the figure.

(iii) **Internal Rotation Barrier of Ethane.** The origin of the internal rotation barrier of ethane has been a subject of extensive studies by means of various theoretical methods.[8,9,21,22] Among these, Hellmann–Feynman force calculations have been made by Goodisman[8] and Sovers, *et al.*[9] Goodisman's torque method resulted in a rather small value, 1–2 kcal/mol, in comparison with the experimental one, 2.875 kcal/mol.[21a] He stressed the importance of the polarization of the electron cloud near the proton. The force difference method proposed by Sovers, *et al.*,[9] yields fairly good values. They concluded that the repulsion between C–H bonds in ethane is similar to that between two helium atoms. Similar conclusions were also reported by Allen.[23] Previously, one of the authors[1c] considered the origin of internal rotation barriers about single bonds using the ESF theory. Here, we examine the internal rotation barrier of ethane in more detail.

Figure 3 gives the analysis of the rotational force acting on the proton in ethane. The analyses are made based on eq 7 and 9. The direction of the force F_H and the rotational angle ψ are defined in the illustration shown in the figure. A positive force corresponds to the restoring force *to* staggered form (repulsive force). As seen from the total force curve, the staggered form is calculated to be more stable than the eclipsed form. By integrating the total force curve, we obtained the rotational barrier of 2.4 kcal/mol (experiment 2.875 kcal/mol).

The partitioning of force due to eq 7 (dotted line) shows that the electronic part is attractive but is smaller than the repulsive nuclear part. In the second par-

(21) For comprehensive literature, see the following reviews: (a) J. P. Lowe, *Progr. Phys. Org. Chem.*, **6**, 1 (1968); (b) L. C. Allen, *Annu. Rev. Phys. Chem.*, **20**, 315 (1969).

(22) (a) O. J. Sovers and M. Karplus, *J. Chem. Phys.*, **44**, 3033 (1966); (b) R. M. Stevens, *ibid.*, **52**, 1397 (1970).

(23) L. C. Allen, *Chem. Phys. Lett.*, **2**, 597 (1968).

titioning of force based on eq 9 (real line), the EC(H–C) force becomes the dominant force; although the EC(H–C) force is a minor component of the electronic part, it becomes dominant in the partitioning expressed by eq 9. This force arises from incomplete following of the H–C bond orbital as the nuclei are rotated from staggered to eclipsed forms,[20] which may be illustrated as

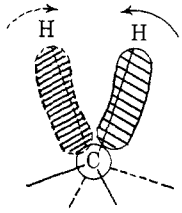

Thus, the orbital following discussed in paper III is found to occur even in ethane. The EC(other) force is composed of nonbonded H–H interactions and also acts as a repulsive force.

It is noteworthy that both of these EC(H–C) and EC(other) forces can be derived from the repulsive exclusion of two approaching C–H bond orbitals. The situation is analogous to the interaction of two helium atoms.[9,23] For the EC(other) forces, the analogy may be trivial. For the EC(H–C) force, some discussion is necessary. When the C–H bond orbitals in each methyl group of ethane approach each other by the rotation from staggered to eclipsed forms, the repulsive exclusion between these C–H bond orbitals causes a distortion of these bond orbitals as illustrated in the above figure. This distortion is nothing else than the orbital incomplete following and causes the repulsive EC(H–C) force.[22]

On the other hand, the EGC force is very small throughout the rotation as seen from Figure 3. This means that the nuclear charge is shielded completely by the negative electron population around it.

Dimerization Reaction of Two Methyl Radicals

The present approach is also applicable to chemical reactions. In paper I, we have pointed out the possibilty that the ESF theory can predict not only the reaction path but also the structural change of reactants along the reaction path (or the structure of the interacting molecules at the transition state). For the dimerization reaction of two methyl radicals, some intuitive discussions have been given. Here, we examine this reaction in more detail and point out some new aspects of the reaction.

In the following sections, two reaction paths are examined. First, two methyl radicals are brought together with their configurations retained rigidly planar. Next, we take account of the freedom of the out-of-plane bending of each methyl radical. The HCH angles are adjusted at every point along the reaction path so that the bending force acting on protons vanishes. A comparison of the results obtained for these two reaction paths reveals the importance of structural changes of the reactants in the course of the reaction.

(i) **Planar Approach.** In this section, two methyl radicals are brought together face to face with their configurations retained rigidly planar. Their relative orientation is chosen as staggered and their C_{3v} axes are held in common throughout the reaction.

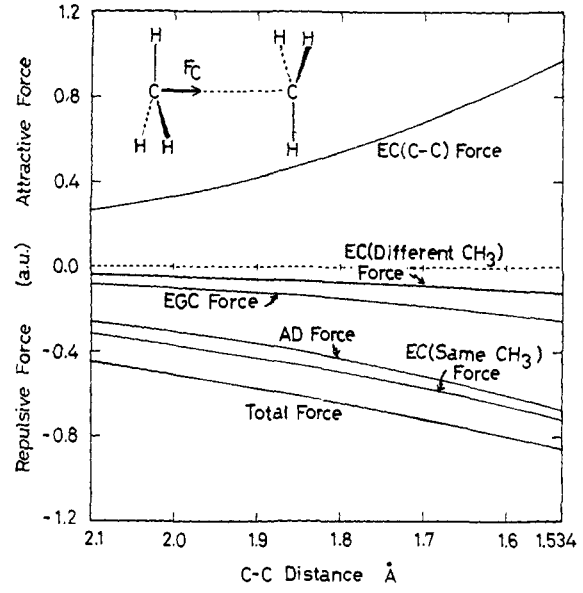

Figure 4. Analysis of the force F_C acting on the carbon when two *planar* methyl radicals approach each other.

Figure 4 shows the dependence of the force acting on carbon upon the intermethyl separation. The analysis of force is based on the partitioning given by eq 8. The positive region corresponds to an attractive force and the negative region to a repulsive force. As seen from Figure 4, the (total) force acting on carbon is repulsive at all the C–C distances studied here. Therefore, the present calculation shows that two methyl radicals cannot dimerize, if they are restricted to be planar in the course of the reaction. This finding corresponds well to the experimental fact that the following radical I

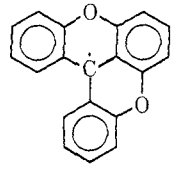

I

which is restricted to be planar by the linkage in the nuclear framework, is stable and 100% dissociated.[24]

As seen from the analysis of force shown in Figure 4, only the EC(C–C) force is attractive in whole stages of the interaction. All of the other components are repulsive throughout the interaction. This shows that, although the electron cloud is accumulated by the interaction in the intermediate region between carbons of two methyl radicals, it is insufficient to drive the reaction. Among the repulsive forces, the relatively important AD and EC(same CH_3) forces are due mainly to the reorganization of the electron cloud within each methyl radical. The repulsive AD force shows that the s–p hybridization at one carbon directs outward from the other methyl radical. The repulsive EC(same CH_3) force shows that the C–H bond orbitals do not lie on the internuclear C–H axes but are distorted outward from another methyl radical. This point is discussed more fully later. The repulsive EC(different CH_3) force is due to the decrease in electron

(24) O. Neunhoeffer and H. Haasse, *Chem. Ber.*, 91, 1801 (1958).

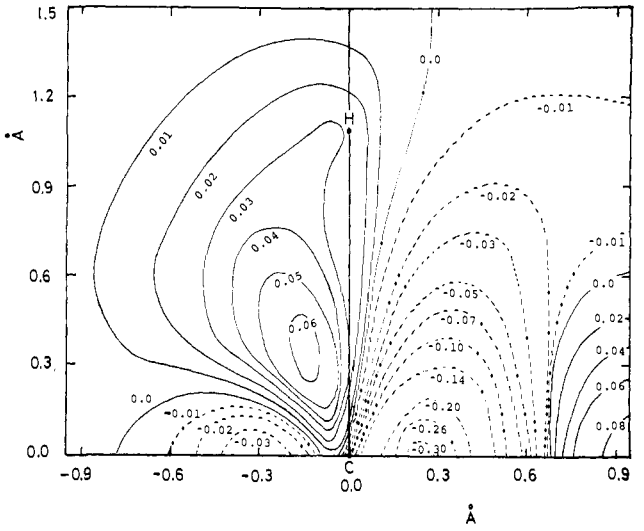

Figure 5. Change in electron distribution induced by the interaction of two planar methyl radicals separated by 1.9 Å. The electron density obtained for two free methyl radicals separated by 1.9 Å is subtracted from the electron density obtained for interacting two planar methyl radicals at the same distance. The map is given on the H–C—C plane and corresponds to the left-hand-side methyl radical.

density in the region between carbon on one methyl radical and protons on the other methyl radical. This is analogous to the interaction of two helium atoms. The repulsive EGC force shows approximately an incomplete shielding of nuclear charges by the electron population around the nuclei.

Next, let us consider the forces acting on *protons* of each methyl radical in the course of the planar approach. Table IV summarizes the force acting on the proton

Table IV. Bending Force Acting on Proton When Planar Methyl Groups Approach Each Other (au)[a,b]

C–C distance, Å	Force			
	Total	EC(H–C)	EC(other)	EGC
2.5	0.018	0.007	0.001	0.010
2.1	0.030	0.013	0.004	0.014
1.9	0.041	0.017	0.007	0.017
1.534	0.074	0.029	0.018	0.027

[a] The direction of force is perpendicular to the C–H axis as

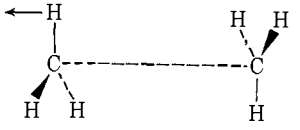

[b] The AD force is always zero in the present calculation.

which is perpendicular to the C–H axis. The analysis of force is based on eq 9. As seen from the total force shown in Table IV, the protons of each planar methyl radical receive the forces that operate to bend each methyl radical outward from each other. This bending force increases with decreasing intermethyl separation. Therefore, it is concluded that each methyl radical becomes nonplanar as two methyl radicals approach each other.

Among the components of this bending force shown in Table IV, the EC(other) and EGC forces arise from the repulsive (nonbonded) interactions of protons in one methyl radical with the carbon and hydrogens in the other methyl radical, while the EC(H–C) force is due to the distortion of the C–H bond orbital. Namely, by the interaction of two planar methyl radicals, the electron distribution in the C–H bond region is reorganized as illustrated by

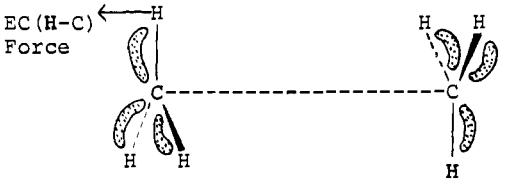

This distortion of the C–H bond orbital produces the EC(H–C) force shown by the arrow. The repulsive EC(same CH_3) force acting on the carbon discussed in the previous paragraph is also due to these bent C–H bond orbitals. Since the displacement of the C–H bond orbitals shown above precedes the bending displacement of the protons, this reorganization of the electron cloud is nothing else but the orbital preceding[20] defined in paper III. Figure 5 shows the change in electron distribution induced by the interaction of two planar methyl radicals separated by 1.9 Å. The map is calculated from the EH MO's and corresponds to the left-hand-side methyl radical of the above figure. The section is the H–C—C plane. The increase in electron density in the back-side region of the C–H axis shows the bond-orbital preceding illustrated in the above sketch. The accumulation of electron density in the intermediate region between two methyl radicals is the origin of the attractive EC(C–C) force shown in Figure 4.

(ii) Gradually Bending Approach. In the above section, it was found that each methyl radical becomes nonplanar as two methyl radicals approach each other. Therefore, here we take the freedom of the out-of-plane bending of each methyl radical into account. The HCH angles are adjusted at every separation so that the bending force acting on protons vanishes. Other conditions are the same as those in the above section.

Table V shows the driving force of the reaction acting

Table V. The Reaction Path and the Driving Force for the Dimerization Reaction of Two Methyl Radicals

C–C distance, Å	Shape along reaction path: θ,[a] deg	HCH angle, deg	Driving force on carbon, au
∞	0.0	120.0	0.000
2.1	10.3	116.8	0.023
1.9	13.0	115.1	0.011
1.8	14.6	113.8	0.007
1.7	16.3	112.4	0.003
1.65	17.2	111.7	0.002
1.584	18.3	110.6	0.001
1.534	19.2	109.8	0.000

[a] θ is the out-of-plane angle of each methyl radical defined in Figure 2.

on the carbon of each methyl radical[25] and the adjusted HCH angles at various separations along the

(25) Since the center of gravity of each methyl radical is very near to the position of carbon, we call the force acting on carbon the driving force of the reaction. The forces acting on protons in the same direction as the reaction coordinate are very small throughout the reaction.

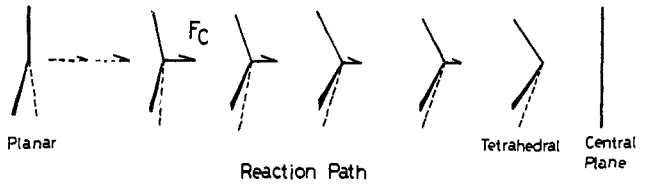

Figure 6. Illustrations of the driving force F_C acting on the carbon and the process of the reaction summarized in Table V. Another methyl radical is at the mirror image position with respect to the central plane.

path. Figure 6 gives an illustration of the driving force F_C and the process of the reaction summarized in Table V. A marked difference of the present results from those obtained for the planar approach is that the force acting on the carbon is *attractive* in all stages of the interaction. This force is nothing else but the driving force of the reaction.[25] It decreases gradually as the reaction proceeds and vanishes when the reaction is completed. Of course, it vanishes also at infinite separation (two free methyl radicals). At the same time, as the reaction proceeds, the HCH angles of each methyl radical shut gradually from planar (in the free methyl radical) to nearly tetrahedral configuration. In comparison with the results of the previous section, it is obvious that this structural change along the reaction path plays an essential role for occurrence of the reaction.

Next, let us consider how each methyl radical acquires an attractive force through this bending along the reaction process. Figure 7 shows the analysis of the driving force acting on the carbon. The definitions and the scale in Figure 7 are the same as those in Figure 4. A comparison of these two figures shows that there are marked differences in the behavior of the AD and EGC forces. These forces are repulsive in the planar approach, while they are attractive in the present gradually bending approach. Among all, the most important change in the AD force shows that the bending of each methyl radical changes the direction of the s–p hybrid at carbon so that it becomes oriented to the other methyl radical. Since the extent of hybridization is very sensitive to the valence angle,[1a] the result is reasonable. As seen in Figure 7, the contribution of the attractive AD force is important especially at relatively large separation (perhaps also at separations larger than 2.1 Å).[26] The change in the EGC force is due to the decrease in nuclear repulsions between the carbon on one methyl radical and protons on the other methyl radical. For other force components, the curves of the EC(C–C) and EC(different CH_3) forces in Figure 7 are almost superimposable on the corresponding curves in Figure 4. Especially, the EC(C–C) force is the most important attractive force also in the present gradually bending approach. On the other hand, the magnitude of the EC(same CH_3) force is different between these two figures. It is more repulsive in the gradually bending approach than in the planar approach. This is due to the fact that in the former approach, the vector sum of the three EC(C–H) forces acting on the carbon within each methyl radical increases repulsively with the increasing extent of bending along the reaction path.

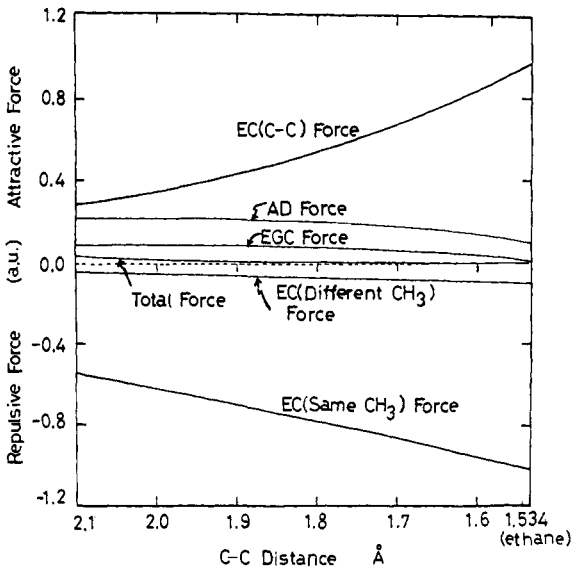

Figure 7. Analysis of the driving force F_C acting on carbon along the reaction path shown in Figure 6 and Table V.

(iii) **Summary**. From the examinations given in paragraph i and ii, the following picture of the dimerization reaction of two methyl radicals may be obtained. Although the interaction of two *planar* methyl radicals induces an accumulation of electron density in the C–C region (Figure 5), it is insufficient to drive the reaction (Figure 4). The interaction also produces a bending force on protons due partly to the orbital preceding of the C–H bond electron cloud (Table IV and Figure 5). The resulting bending of each methyl radical changes the direction of the atomic dipole at carbon so that it becomes oriented to the other methyl radical.[27] The AD force due to this atomic dipole operates as one of the important attractive forces especially in the initial stage of the reaction (Figure 7). The change in the EGC force is also favorable for the occurrence of the reaction. The EC(C–C) force, which is the most important attractive force (Figure 7), suffers little change by this bending. Thus, the bending of each methyl radical facilitates the occurrence of the reaction. The reaction proceeds accompanying a change in valence angles at carbon (Figure 6).[28] If the planarity is forced by other restrictions (as in radical I given in the previous paragraph), the dimerization reaction cannot proceed. These results show that the geometrical change of the reactants along the reaction path is essential for occurrence of the reaction.

Concluding Remarks

As mentioned at the outset of this report, the present study was begun as a trial for the use of semiempirical wave functions for the calculation of electrostatic forces. Although some difficulties still remain for

(26) The ratio of the AD force to the EC(C–C) force is 0.83 at the C–C separation of 2.1 Å and 0.12 at 1.534 Å (the equilibrium C–C distance of ethane).

(27) This formation of atomic dipole is a kind of orbital preceding near the reaction site. A marked characteristic of this orbital preceding lies in the fact that it is induced through the change in geometry of the reactant in the course of the reaction. It is not a direct consequence of the interaction of two methyl radicals

(28) As seen from Table IV, the bending of each methyl radical contributes to stabilize the energy of the interacting system. Therefore the present calculation shows that there is no activation barrier for the dimerization reaction of two methyl radicals.

general quantitative utility, the present results seem to be satisfactory as a whole. Among all, what is most important seems to be the intuitiveness of the force concept, which is shown in the analyses of forces for molecular structure and chemical reactions by means of the ESE theory proposed previously.[1] The importance of the AD and EC forces is confirmed. The EGC force is less important for the cases studied here. Some important features of the electron density distribution (orbital following and preceding) in the course of nuclear displacements are also pointed out.[20,27]

Note lastly that if the density matrix P_{rs} in eq 3 is determined by some appropriate quantum-mechanical method, the computational time necessary for the calculation of force is nearly the same for any wave function. If we use wave functions which satisfy the Hellmann–Feynman theorem, the total results should be the same from both energetic and electrostatic force standpoints. However, since the latter standpoint seems to have more conceptual utility than the former, we recommend its use jointly with the former.

Acknowledgments. We acknowledge Professor T. Yonezawa for his encouraging interest in this study and Professor H. Kato and Dr. T. Kawamura for their helpful suggestions. We also thank the members of the Quantum Chemistry Group of their department for active discussions and the referees for helpful suggestions. Lastly, we wish to express our appreciation to the Data Processing Center of Kyoto University for generous use of the FACOM 230-60 computer.

Circular Dichroism of Cobalt(II) Complex between 1700 and 1200 cm^{-1}. Observation of Spin–Orbit and Tetragonal Field Splitting of the $^4T_{1g}$ Ground State Manifold

Edward C. Hsu and G. Holzwarth*

Contribution from the Departments of Chemistry and Biophysics, The University of Chicago, Chicago, Illinois 60637. *Received May 2, 1973*

Abstract: Measurements of the room temperature circular dichroism (CD) of the dimer of bis[3-(trifluoromethylhydroxymethylene)-*d*-camphorato]cobalt reveal six bands between 1680 and 1200 cm^{-1}. The observed CD is assigned to electronic transitions of Co^{2+} from the ground and first excited Kramers doublets to the higher Kramers levels of the $^4T_{1g}$ ground manifold, which is split by spin–orbit coupling and a ligand field of tetragonal symmetry.

The circular dichroism of transition metal compounds yields valuable information on the nature of their electronic states.[1–9] Strong CD bands in the optical and near-infrared range are often used as evidence for magnetic dipole allowed transitions of the metal ion from a ground spin multiplet to excited levels of the same spin multiplicity. For systems where the major field is highly symmetric, for example, having symmetry O_h or T_d, each spin multiplet may have orbital degeneracy. Due to the spin–orbit interaction and the minor ligand field of lower symmetry, each energy level will split into sublevels. However, the observed room temperature CD of solutions usually does not reveal this sublevel structure. Indeed, even low temperature single crystal CD studies have not revealed spin–orbit splitting, as shown, for example, by Meredith and Palmer[10] for the $^3A_{2g} \rightarrow {}^3T_{1g}$ transition of Ni^{2+} in α-$NiSO_4 \cdot 6H_2O$.

An alternative method for studying this spin–orbit splitting is the measurement of CD for transitions among the sublevels of the ground state spin multiplet. The wavelength of the light inducing such transitions falls into the infrared range. This paper reports the observation of such electronic infrared circular dichroism of bis[3-(trifluoromethylhydroxymethylene)-*d*-camphorato]cobalt measured at room temperature in CCl_4 solution between 900 and 5000 cm^{-1}.

Experimental Section

Ligand. The ligand 3-(trifluoromethylhydroxymethylene)-*d*-camphor, hereafter abbreviated tfhmc, was synthesized by the condensation of *d*-camphor with trifluoroacetyl acetonate following the method of Kopecky, *et al.*[11] The infrared absorption spectrum of a film of the ligand showed a broad band at 3350 cm^{-1} (O—H stretch), two strong peaks at 1745 and 1705 cm^{-1} (C=O stretching modes), and a relatively strong band at 1650 cm^{-1} (C=C stretch of the enol form), in addition to the bands expected from the camphor skeleton and the CF_3 group. These data agree with the ir study by Lintvedt and Fatta[12] on methylhydroxymethylene-*d*-camphor and are those expected for a β-diketone.

Complexes. Complexes of tfhmc with the ions Co^{2+}, Ni^{2+}, Cu^{2+}, and Fe^{2+} were prepared by dissolving the tfhmc in an ethanol:water mixture (7:3 v/v), adjusting the pH to 6–7, and adding to this mixture a solution of $Co(NO_3)_2$, $Ni(NO_3)_2$, $CuCl_2$, or $FeCl_2$ in the same ethanol:water solvent.[13] Evaporation of the ethanol caused precipitation of the complex. The product was filtered, redissolved

(1) W. Moffitt, *J. Chem. Phys.*, **25**, 1189 (1956).
(2) S. Sugano, *J. Chem. Phys.*, **33**, 1883 (1960).
(3) N. K. Hamer, *Mol. Phys.*, **5**, 340 (1962).
(4) T. S. Piper and A. Karipides, *Mol. Phys.*, **5**, 475 (1962).
(5) A. J. McCaffery and S. F. Mason, *Mol. Phys.*, **6**, 359 (1963).
(6) R. M. King and G. W. Everett, Jr., *Inorg. Chem.*, **10**, 1237 (1971).
(7) F. Richardson, *J. Chem. Phys.*, **54**, 2453 (1971).
(8) F. Richardson, *J. Phys. Chem.*, **75**, 692 (1971).
(9) A. D. Liehr, *J. Phys. Chem.*, **68**, 665, 3629 (1964).
(10) P. L. Meredith and R. A. Palmer, *Chem. Commun.*, 1337 (1969).
(11) K. R. Kopecky, D. Nonhebel, G. Morris, and G. S. Hammond, *J. Org. Chem.*, **27**, 1036 (1962).
(12) R. L. Lintvedt and A. M Fatta, *Inorg. Chem.*, **7**, 2489 (1968).
(13) K. J. Eisentraut and R. E. Sievers, *J. Amer. Chem. Soc.*, **87**, 5254 (1965); G. Whitesides and D. W. Lewis, *ibid.*, **92**, 6979 (1970).